Supporting information for

Computational Description of Key Spectroscopic Features of Zeolite SSZ-13

Florian Göltl[1,2,], Alyssa M Love[1], Sarah C. Schuenzel[2], Patrick Wolf[1], Manos Mavrikakis[2,*], Ive Hermans[1,2,*]*

[1] Department of Chemistry, University of Wisconsin – Madison, 53706 Madison, WI, USA Department of Chemical and Biological Engineering, University of Wisconsin – Madison, 53706 Madison, WI, USA

[2] Department of Chemical and Biological Engineering, University of Wisconsin – Madison, 53706 Madison, WI, USA

e-Mail: fgoeltl@wisc.edu, emavrikakis@wisc.edu, hermans@chem.wisc.edu

S1: Choice of cell volume

The protonated case: As a first step we optimize the cell volume for all the studied sites. We systematically varied the unit cell volume over a range from 770 Å^3 and 870 Å^3 and used a square fit to determine the minimum (see Table S1). We find a significant dependence of the different Al and defect distributions. The cell volume in general increases with the Amount of Al in the unit cell (811 Å^3 for 0Al, 823.8 Å^3 for 1Al and ~837 Å^3 for 2Al). Furthermore the defect site is also at a volume of 822.3 Å^3. These values agree reasonably well with reports in the literature and small differences are expected due to differences in the computational setup. If the zeolite would be perfectly periodic and would only consist of one type of unit cell, the choice of unit cell volume would be simple. However, in a realistic zeolite system a distribution of local Al and defect configurations will be present and the unit cell volume will most likely be an average over the Al configurations present. Since most of the work for SSZ-13 focuses on materials with Si/Al ratios above 6 and below 15, we make a compromise and choose a unit cell volume of 830 Å^3 in all our calculations. However, the real unit cell volume might change based on the Si/Al ratio and it might be necessary to adapt the chosen unit cell volume.

Table S1: *Optimized unit cell volume for protonated Al configurations in SSZ-13*.

Site	Volume [Å^3]
Si-SSZ13	811
$1Al_1$	823.8
$2Al^A{}_{1\text{-}1}$	840.6
$2Al^B{}_{1\text{-}1}$	837.7
$2Al^C{}_{2\text{-}1}$	837.5
$2Al^D{}_{1\text{-}1}$	836.8
$2Al^E{}_{1\text{-}1}$	833.0
d^4	822.3
$d^3{}_2$	810.3

Unit cell volumes for a uniform background charge: In a subsequent step we optimized unit cell volumes for systems with a uniform background charge used for NMR calculations. Now we vary the cell volume between 800 Å^3 and 900 Å^3. For all sites we find a significant expansion to 836.5 Å^3 for 1Al and ~862 Å^3 for the 2 Al cases. This expansion is consistent with experimental measurements, which find an expansion of the unit cell volume upon hydration. Following a similar logic as above, we choose a unit cell volume of 860 Å^3.

Table S2: *Optimized unit cell volumes for Al configurations with a uniform background charge*.

Site	Volume [Å^3]
1Al	836.5
2Al^A	862.8
2Al^B	862.4
2Al^C	861.5
2Al^D	863.6
2Al^E	862.7

S2: Occupational probabilities for $2Al^{A}$-$2Al^{E}$ and d

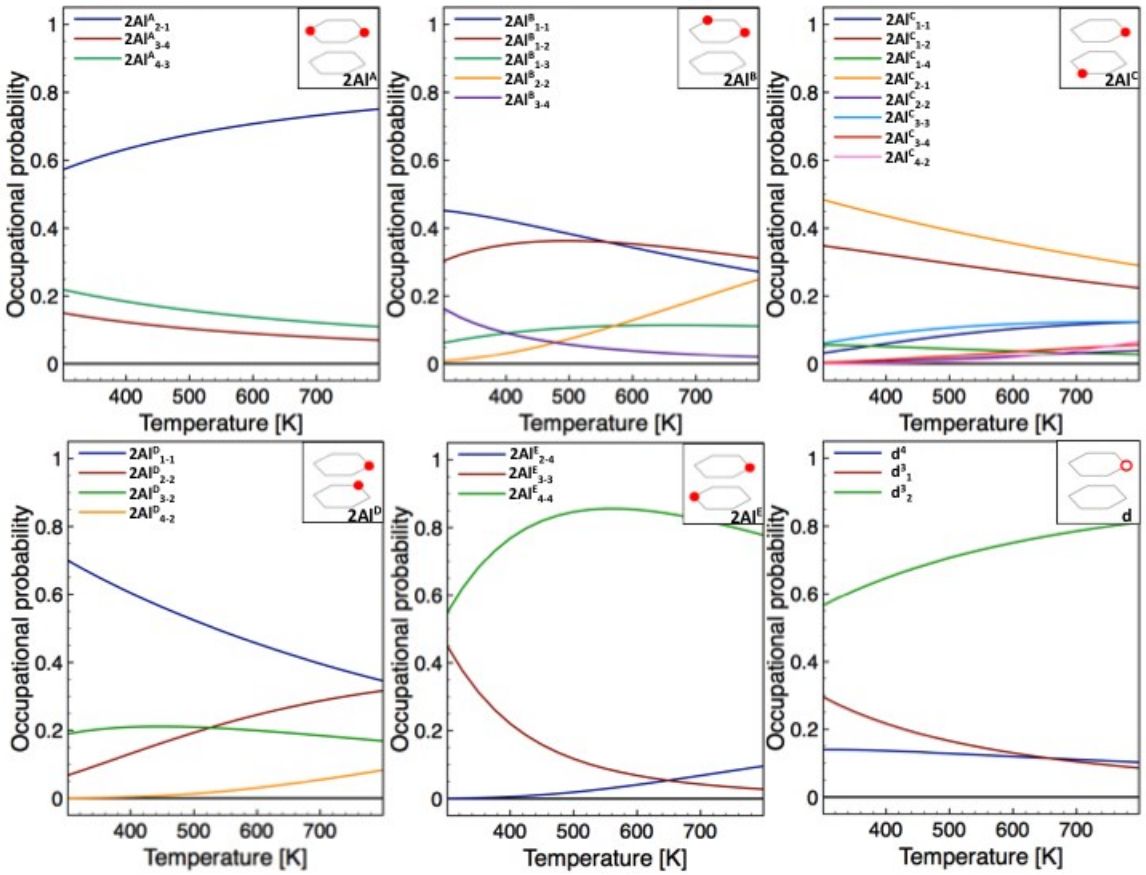

Figure S1: *Occupational probabilities for Al configurations $2Al^{A}$ through $2Al^{E}$ and d as shown in Fig 1 A. Occupational probabilities were calculated using Boltzmann weights; details are given in the main text. Sites with occupations below 0.05 were omitted for clarity.*

S3: Defect sites at 830 Å^3

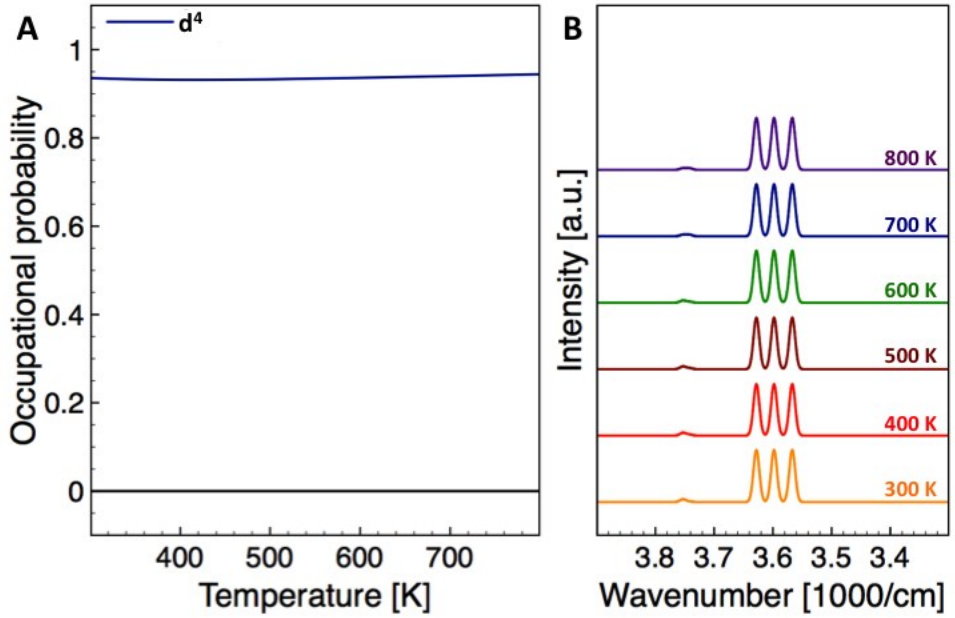

Figure S2: *A: Occupational probabilities for the defect site at a cell volume of 830 Å^3. Occupations below 0.05 were omitted for clarity of the plot. B:Temperature dependent OH vibrational spectrum for the defect sites at a cell volume of 830 Å^3.*

S4: Finite temperature IR spectra of the different Al configurations.

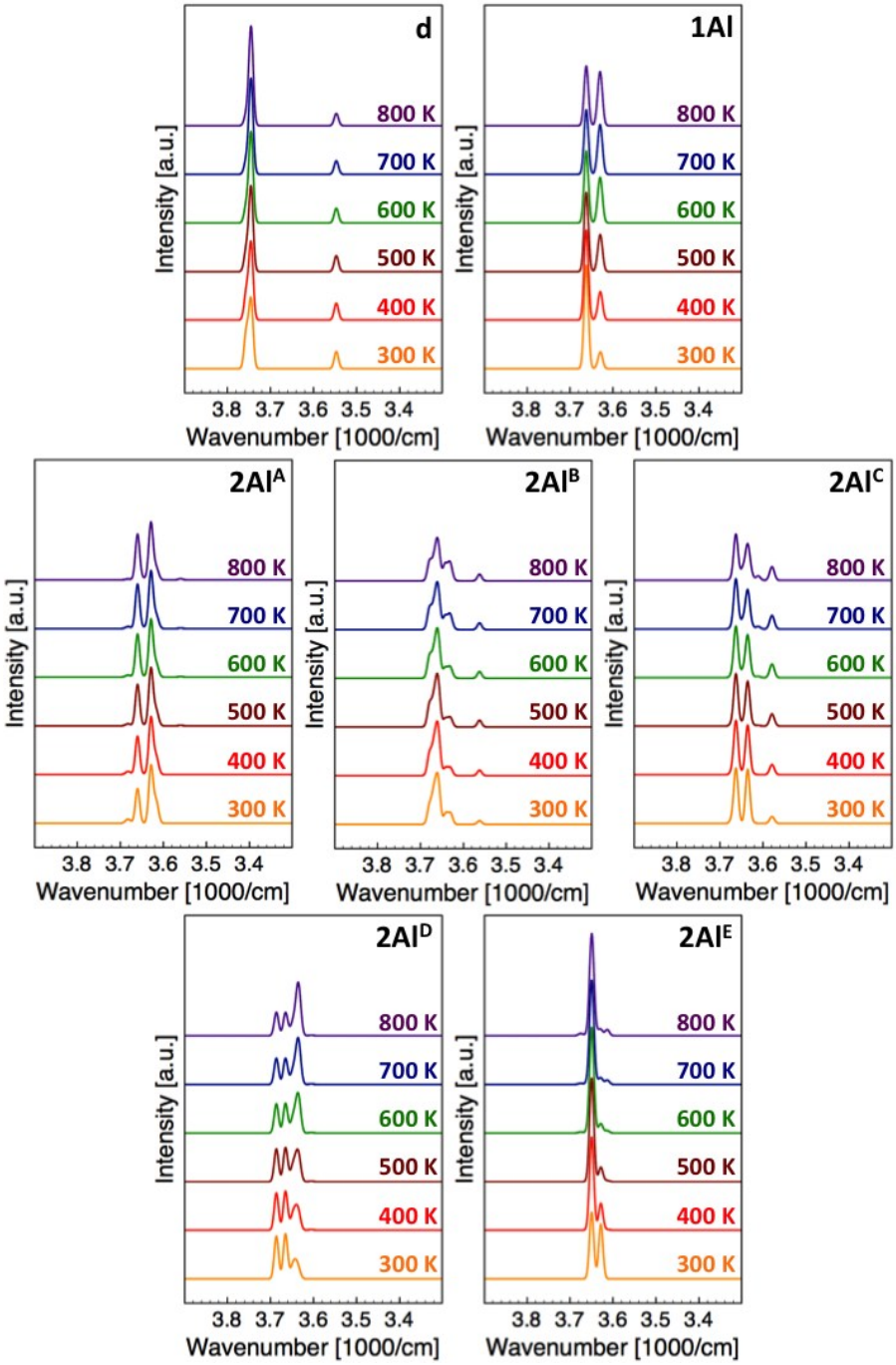

Figure S3: *Temperature dependent OH IR spectra for the different Al distributions and defect site in the zeolite SSZ-13.*

S5: Spectra and intensities for OH-vibrational spectra for the defect site

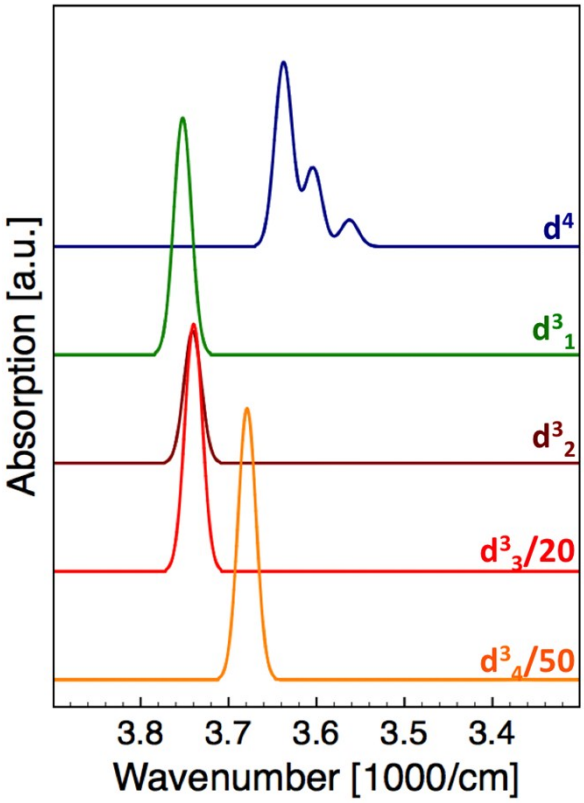

Figure S4: *Spectra for the d site at 810 Å³ calculated using dipole transition moments for intensity. As can be seen in particular for the d^3 sites only the highest vibrational frequency contributes. To the observed spectral intensity. Spectra for d^3_3 and d^3_4 were scaled to arrive at a similar intensity scale. In the calculations of the d site at 830 Å³ similar trends are observed. However, for the d^4 site three transitions showed similar intensities. We therefore included the three highest wavenumbers in the calculation of the spectrum of d^4 in Fig. S2 B.*

S6: Temperature dependent ^{27}Al-NMR spectra for the protonated zeolite

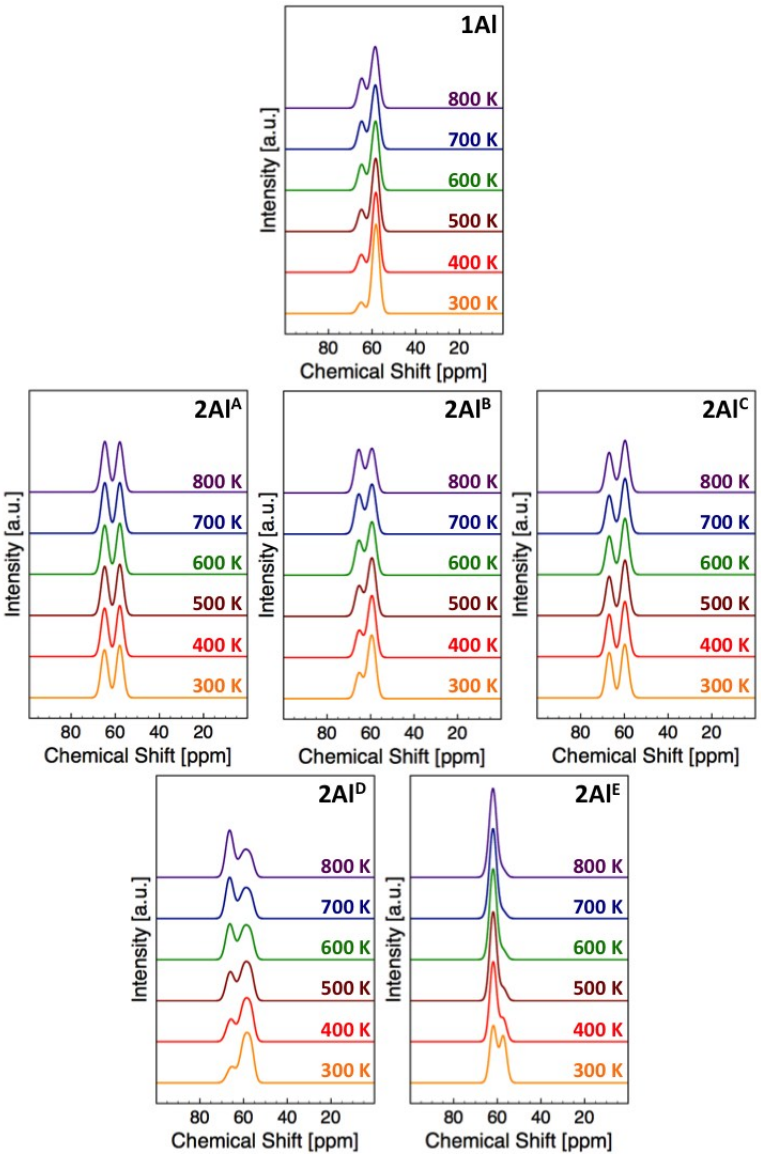

Figure S5: *Temperature dependent ^{27}Al-NMR spectra for the different Al configurations. Each Al configuration leads to a distinct multi-peak spectrum, which is not observed experimentally. Spectra were calculated using Boltzmann probabilities displayed in Fig. 2 of the main text and given in the Supporting Data File.*

S7: ^{29}Si-NMR and ^{27}Al-NMR isotropic chemical shifts for the hydrated sample

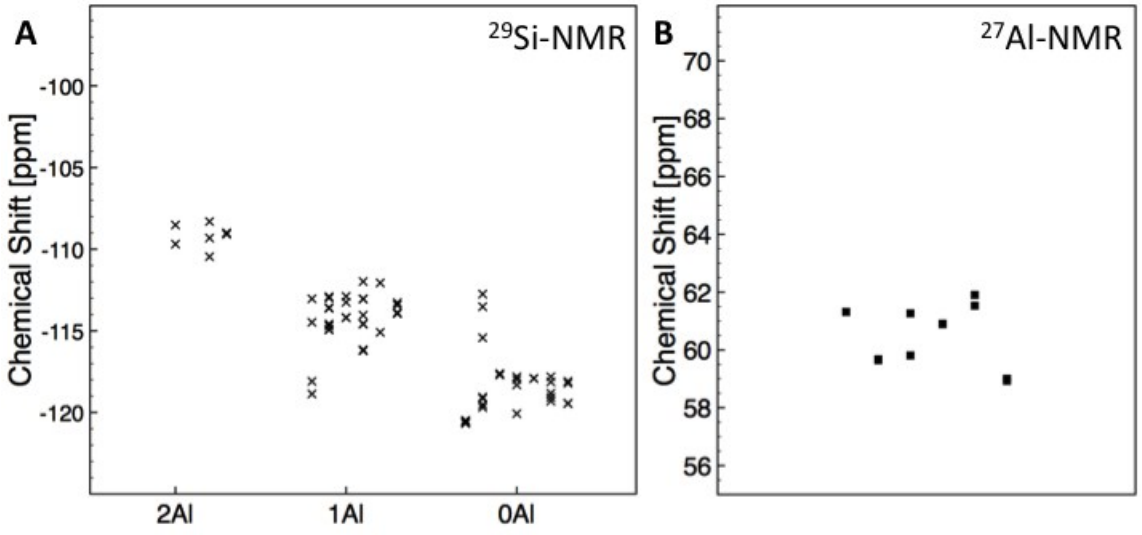

Figure S6: *A: ^{29}Si-NMR isotropic chemical shifts calculated for all modeled SSZ13 structures using a uniform background charge. B: ^{27}Al-NMR isotropic chemical shifts calculated for all modeled SSZ13 structures using a uniform background charge. Columns of data represent (from left to right) 1Al, 2Al^{A}-2Al^{E}. Numerical values for isotropic chemical shifts are given in the Supporting Information.*

S8: ^{27}Al-NMR spectrum

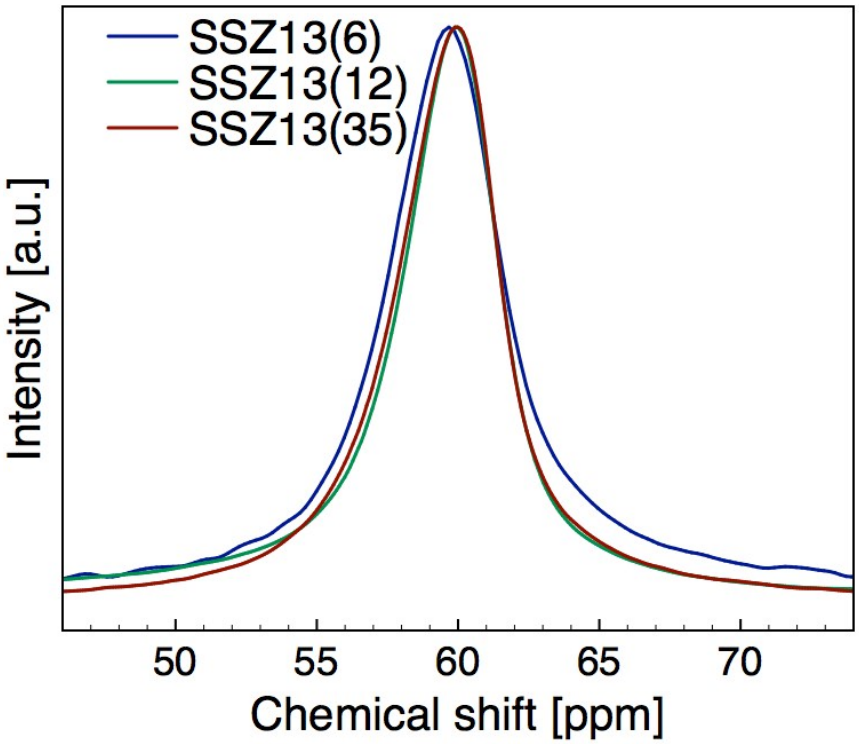

Figure S7: Comparison of ^{27}Al isotropic chemical shifts for SSZ13(6) (blue), SSZ13(12) (green) and SSZ13(35) (red).

S9: Occupational probabilities and temperature dependent OH-IR spectra for the large unit cell

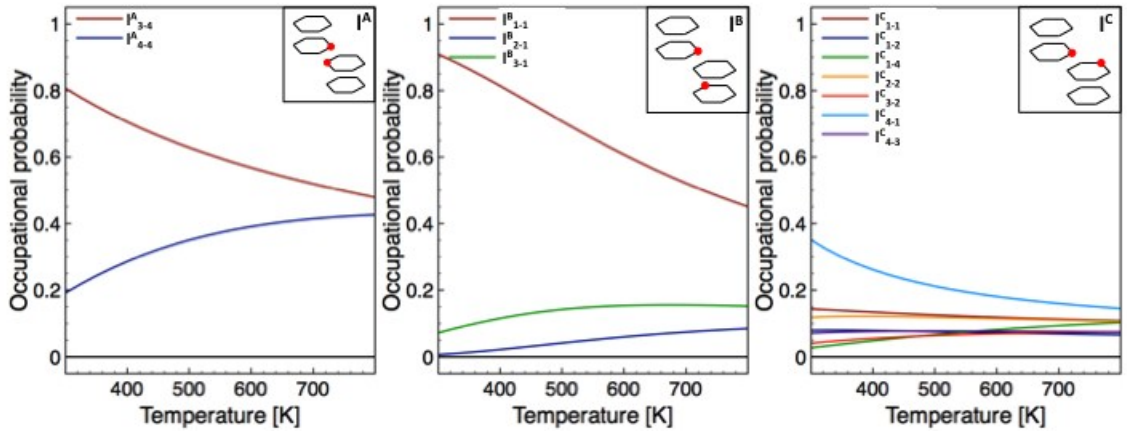

Figure S8: *Occupational probabilities for different proton positions for the local Al and defect distributions shown in Fig 8 of the main text. Occupational probabilities were calculated using Boltzmann weights and the details are given in the main text. Sites with occupations below 0.05 were omitted for clarity.*

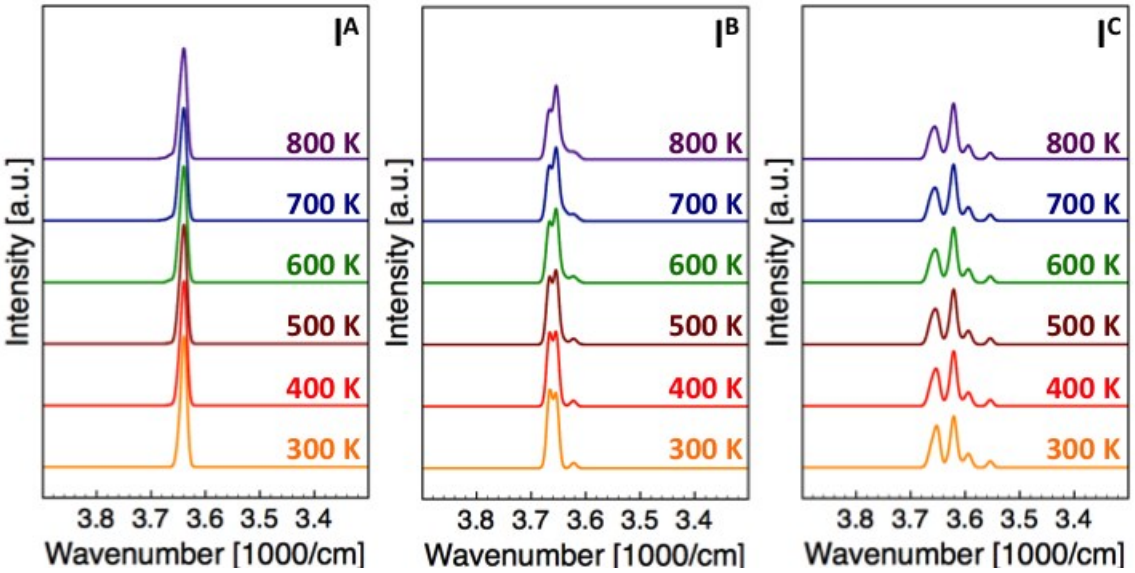

Figure S9: *Temperature dependent OH-IR spectra for the different Al configurations of the large unit cell shown in Fig. 8 of the main text. Each Al configuration leads to a distinct multi-peak spectrum, which is not observed experimentally. Spectra were calculated using Boltzmann probabilities displayed in Fig. S5 and given in the Supporting Data File*

S10: Impact of energy cut-off

In this paper we use an energy cut-off of 420 eV to model the zeolite structures. Here we test the impact of an increase in the energy cut-off to 600 eV for the 1Al configuration. As a first step we test the relative energies calculated at the higher energy cut off (see Tab. S3). As can be seen we find relative energies within 0.001 eV. This indicates that an energy cut-off of 420 eV is an accurate choice for relative energies. In a next step we focus on OH-IR vibrational frequencies. Here we observe a blue shift of ~40 cm^{-1} in all wavenumbers. However, differences in wavenumbers between proton positions are again well reproduced.

Table S3: Relative energies (ΔE), wavenumbers (ν) and relative wavenumbers (Δν) for the 1Al configuration calculated at 420 eV and 600 eV. Relative energies and relative wavenumbers are given with respect to $1Al_1$.

	ΔE [eV]		ν [cm^{-1}]		Δν [cm^{-1}]	
	420 eV	600 eV	420 eV	600 eV	420 eV	600 eV
$1Al_1$	0.000	0.000	3662	3701	0	0
$1Al_2$	0.052	0.053	3628	3669	-35	-32
$1Al_3$	0.085	0.086	3633	3673	-29	-28
$1Al_4$	0.099	0.098	3628	3665	-34	-36

Based on this data we see our choice of an energy cut-off of 420 eV justified. Relative trends are well reproduced and absolute values for wavenumbers agree better with experimental measurements. We attribute this improved agreement with experiments in terms of wavenumber to partial error cancelation in terms of energy cut-off (blue shift) and neglect of anharmonic correction (red shift).